Weldability of Hot Isostatically Pressed Prealloyed Titanium 6Al-4V Powder

Rotating electrode process powder is weldable after consolidation by hot isostatic pressing, but hydride-dehydride process powder compacts exhibit linear porosity in the fusion zone and may not be suitable for some applications

BY M. A. GREENFIELD, R. F. GEISENDORFER, D. K. HAGGARD AND L. P. CLARK

ABSTRACT. Hot isostatic pressing of titanium alloy powders to near net shape offers the opportunity for considerable cost reductions through better material utilization. Further savings can be achieved by the welding of these powder compacts into more complex shapes.

This investigation examines the effects of both rotating electrode and hydride-dehydride powder, and compaction parameters on resultant weldability.

Introduction

Although the high strength, light weight and corrosion resistance of titanium alloys make them attractive for aerospace applications, their usage has been limited because of the high cost of component fabrication. Typically, material utilization is low; the ratio of material purchased to material used in the final part is often greater than 10 to 1, as in the manufacture of compressor stub shafts where 170 pound forgings result in 12 pound parts.

At a machining cost of ten to fifteen dollars per pound of metal removed, the cost of many titanium component designs is excessively high and hence impractical. The recent trend, therefore, has been to substitute lower cost but structurally less efficient materials. One approach to reduce component cost and achieve broader aerospace applications for titanium is to exploit existing and emerging powder metallurgical technology.

Powder metallurgy has long been used for the production of low cost components. In general, however, this has been limited to the production of high volume, low stress parts such as iron, steel, and brass components for the automotive and appliance industries. Since the mid-1960s, there have been two prealloyed titanium production processes available to the aerospace industry—the rotating electrode process (REP) and the hydride-dehydride (H/DH) powder process. REP powder is produced by spark melting a rotating titanium alloy bar in an inert gas filled chamber and collecting the spherical powder. In the H/DH process the alloy is hydrided to make it brittle, crushed and later reversibly dehydrided, producing powder of an irregular shape.

Table 1—Chemical Analysis of Ti-6Al-4V Starting Material, Wt-%

Titanium	Balance
Aluminum	6.4
Vanadium	4.2
Iron	0.03
Oxygen	600 ppm
Nitrogen	100 ppm
Hydrogen	100 ppm

In a study of Peebles (Ref. 1) Ti-6Al-4V forging preforms were produced using H/DH powders consolidated by cold pressing and vacuum sintering. The preforms were subsequently conventionally alpha-beta forged to fully dense parts. The program demonstrated that properties equivalent to conventional wrought components could be produced at a considerable cost savings over the current processes. However, GTA and EB welding studies conducted on the forged product showed excessive porosity in the weld heat-affected zones presumably as a consequence of incomplete compaction. A similar study, conducted by Witt and Paul (Ref. 2), produced parallel results except that, in a cursory weld evaluation, the consolidated product could be successfully EB welded, provided that the compacts were fully dense.

Both studies showed that an improved compaction process to that of pressing and sintering was needed to produce a fully dense weldable product with acceptable properties. The hot isostatic pressing (HIP) process was evaluated by Geisendorfer, *et al* (Ref. 3). This process (described below) was shown to be a highly promising consolidation technique for Ti-6Al-4V, yielding a fully dense compact with tensile and toughness properties at least equivalent to their wrought counterparts. A preliminary electron beam weldability check of consolidated REP powder showed no porosity.

A recently completed study by Peebles (Ref. 4) showed that HIP of REP prealloyed Ti-6Al-4V powder produced fully dense forging preforms. An ongoing study by Fleck (Ref. 5) is attempting to demonstrate the capability of producing near net parts for use in the as-HIP condition without secondary working operations and with total cost reductions of up to 50%. It is, therefore, desirable to determine as many applications as possible for applying this developing technology. Since many airframe and engine parts require welding, the powder metallurgy product must be weldable if usage is to be maximized. Although some preliminary work has been done to determine the weldability of consolidated titanium powder, no systematic study has been carried out. There-

Based on paper presented at the AWS 56th Annual Meeting held in Cleveland, Ohio, during April 21-25, 1975.

The work described in this paper was largely accomplished while all four authors were associated with the Air Force Materials Laboratory, Dayton, Ohio.

Fig. 1—Microstructure of starting material. 0.4 in. = 100 μm (reduced 38% on reproduction)

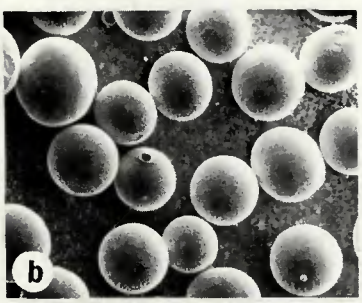

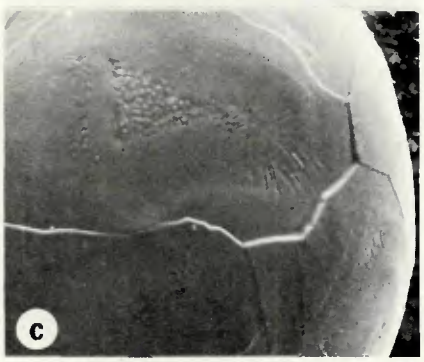

Fig. 2—Microstructures of REP powder: Top (a)—powder cross section, ×100; middle (b)—SEM, ×38; bottom (c)—SEM, ×380 (reduced 32% on reproduction)

fore, this study was undertaken to gain a better understanding of the weld

Table 2—Mechanical Properties of Wrought Ti-6Al-4V Starting Material

	6 in. diameter billet[a]	2½ in. diameter barstock
Ultimate tensile strength:		
ksi	137	125
(MPa)	(945)	(862)
0.2% yield strength:		
ksi	130	110
(MPa)	(896)	(758)
Reduction in area, %	48	47
Elongation in 2 in., %	16	19

(a) Pancake upset 63% at 1750 F (954 C), annealed 1300 F (704 C)—2 h AC

characteristics of the as-HIP product in anticipation of future requirements.

Two prealloyed Ti-6Al-4V powder shapes were investigated: REP spherical powder and H/DH irregular powder. Both types were evaluated after three different time-temperature-pressure HIP combinations. In addition, a fourth HIP cycle above the beta transus was conducted with spherical powder only.

Welding was conducted on as-compacted material using the bead-on-plate gas tungsten arc technique with full penetration and constant weld parameters. Weldments were evaluated by bend, tensile, and toughness testing in conjunction with radiographic, metallographic, and microhardness techniques.

Experimental Procedure

Material

All starting material was from the same heat of Ti-6Al-4V alloy purchased to AMS 4928 except that a low oxygen content (800 ppm maximum) was specified to allow for potential pickup during powder production and handling. The chemistry, mechanical properties and microstructure of the starting materials are given in Tables 1 and 2 and Fig. 1, respectively. Lathe-turned 6 in. (152.4 mm) diameter billets were used for conversion to H/DH powder; whereas, 2½ in. (63.5 mm) diameter centerless ground barstock was used for conversion to powder by the REP.

Spherical powder was produced by rotating the barstock at high speed in a chamber filled with static helium and arc melting the bar with a nonconsumable nonrotating thoriated-tungsten electrode. The molten metal was spun off as small droplets which solidified in flight producing essentially spherical shapes. The powder has a cast microstructure (Fig. 2) with relatively smooth surfaces. The powder size was a function of the speed of rotation of the bar and has a Gaussian size distribution.

Irregular shaped powder was produced by hydriding slices of the billet

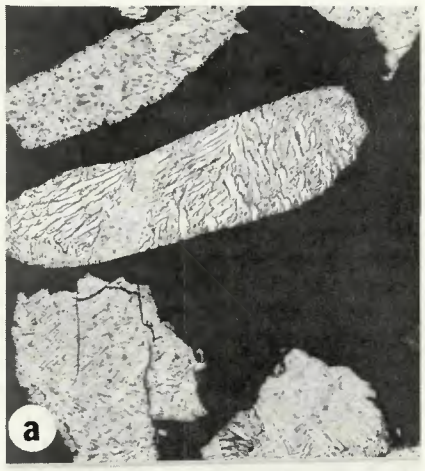

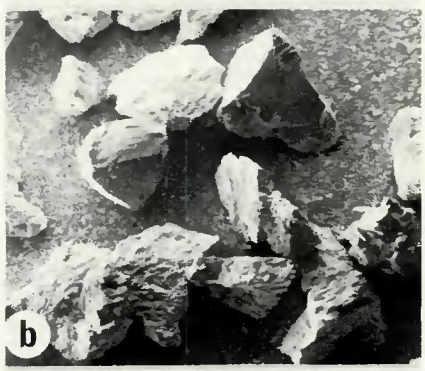

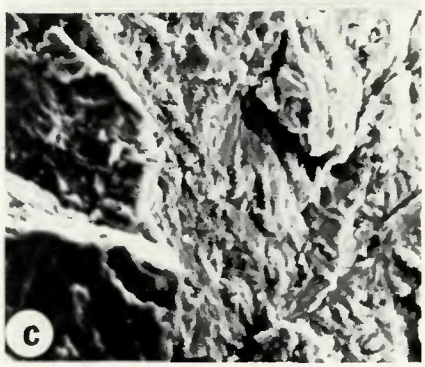

Fig. 3—Microstructure of H/DH powder: Top (a)—powder cross section, ×160; middle (b)—SEM, ×38; bottom (c)—SEM, ×750 (reduced 21% on reproduction)

material at approximately 850 F (454 C) in an hydrogen atmosphere and subsequently cooling and comminuting the

embrittled hydrided titanium alloy via crushing and pulverizing under inert atmosphere. Following sieving and magnetic separation, the powder was dehydrided at 1300 F (704 C) under dynamic vacuum. Powder produced by this method retained the microstructure of the input material—Fig. 3. It was blocky and angular in shape with a relatively high specific surface. Its size distribution was also Gaussian, but the H/DH powder usually contained a higher fraction of finer particles than did the REP powder as shown in Fig. 4.

A full characterization of the starting powders is given in a report by Peebles (Ref. 4).

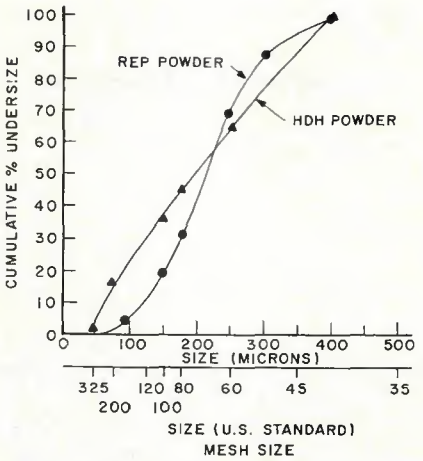

Fig. 4—Powder particle size distribution

Compaction

Powders were canned in mild steel, evacuated, sealed and consolidated by HIP at various time-temperature-pressure combinations. Prior to sealing, cans of REP powder were outgassed for 15 h at room temperature and a manifold vacuum of about 10^{-5} torr (133.32 Pa × 10^{-5}); whereas, cans containing H/DH powder were outgassed at room temperature for 3 h at a manifold vaccum of 10^{-5} torr (133.32 Pa × 10^{-5}) and then hot outgassed at 1000 F (538 C) for 4 h and sealed at the same manifold vacuum.

The outgassing procedures were selected based upon mechanical properties obtained by Peebles (Ref. 4). The vibratory density of the REP powder was 66% and was sufficiently high to prevent excessive wrinkling of the container during consolidation; however, the H/DH powder, with a vibratory density of 51%, required a cold isostatic compaction step to increase the green density to about 60–65% prior to being HIP.

The HIP process used for consolidating powders in this study consisted of first loading the evacuated and hermetically sealed cans of powder into a cold-wall internally resistance heated pressure vessel. The vessel was then evacuated and pressurized with argon gas and heated according to predetermined parameters of time, temperature and pressure.

The seven compacts for this study were selected to cover a range of compaction parameters including a cycle known to yield less than fully dense compacts. The HIP parameters used for both powder types are shown in Table 3. In order to perform weldability tests, the as-received compacts were decanned and machined into flats. Figure 5 shows a typical decanned compact and the final flats obtained.

Welding

Specimens were welded in the as-HIP condition. All specimens were pickled in a HNO_3-HF acid solution prior to welding to remove any surface contamination. Full penetration bead on plate gas tungsten arc welds were made using 10.5 V dcsp, 190 A., and 5.5 ipm (140 mm/min) travel speed (21.8 kJ/in. energy input). Argon was used for the shielding gas at the following rates: 15 cfh (0.42 m^3/h) for electrode holder operation, 30 cfh (0.85 m^3/h) trailing and 15 cfh (0.42 m^3/h) for backing.

Testing

Tensile, face bend, and slow bend Charpy testing along with microhardness measurements were used to characterize the mechanical behavior of the welded HIP powder product. All tests were conducted in laboratory air at room temperature. The face bend specimens (approximately 7 in. long, 1.5 in. wide and 0.10 in. thick, i.e. 177.8 × 38.1 × 2.5 mm) were ground, polished, and pickled to remove any surface contamination occurring after the welding operation. These specimens were bent in the longitudinal direction with the face of the weld in tension.

Guided bend test procedures were followed with the die radii between 2 and 3/4 in. (50.8 and 19 mm). The radius of the die used prior to failure was recorded and the elongation (in 1 in.) measured for each specimen. The longitudinal weld guided bend test was used in order to determine the ductility of the welded samples. This test is preferred since all portions of the weld zone (FZ, HAZ, base metal) are strained equally, thereby giving useful ductility data.

Room temperature tensile tests transverse to the weld bead were conducted with a standard sheet specimen geometry with a 1 in. (25.4 mm) gauge length. Slow bend fracture toughness determinations were made in the heat-affected zone (HAZ) and fusion zone, using precracked 0.125 in. (3.2 mm) thick Charpy V-notch specimens, in conjunction with a Manlabs Model 5B-750 tester at a crosshead speed of 0.1 ipm (2.5 m/min). The load-deflection curves recorded allowed the determination of K_Q values using the methods recommended in ASTM Standard T399 for 3-point bend specimens and rising load conditions.

Results

The results of transverse tensile tests on as-welded REP and H/DH powder consolidated under different compac-

Table 3—As-Welded Properties[a] of Hot Isostatically Pressed Ti-6Al-4V

Compact[b] number	HIP parameters	Density	Yield strength, ksi	Ultimate strength, ksi	Reduction of area, %	Elongation, %	Fracture toughness Base	HAZ	Fusion zone
							ksi $\sqrt{in.}$		
R1	1550 F/10 ksi/2 h	>99.9	124	133	33	10	42	54	54
H/DH5		99.9				Not weldable			
R2	1750 F/10 ksi/1 h	100	113	123	36	11	51	56	55
H/DH6		100	119	132	27	8	48	54	55
R3	1750 F/8 ksi/3 h	100	111	124	38	11	58	53	55
H/DH7		100	120	131	26	11	46	55	58
R4	1750 F/10 ksi/1 h plus 1860 F/10 ksi/½ h	100	111	122	27	10	63	54	56
Wrought	—	100	125	133	30	8	51	56	57

(a) All specimens failed in the base material
(b) R—rotating electrode powder; H/DH—hydride/dehydride powder

Table 4—As-welded Longitudinal Bend Properties

	Radius of die at onset of cracking	Elongation in 1 in., %	Crack initiation site
R1	7.5T	6.7	FZ
H/DH5	Not weldable		
R2	7.5T	7.1	FZ
H/DH6	7.5T	8.6	FZ
R3	10T	5.1	FZ
H/DH7	10T	6.3	FZ
R4	7.5T	7.4	FZ
Wrought	7.5T	9.4	FZ

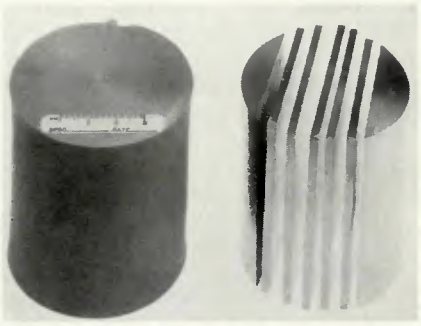

Fig. 5—Decanned compact and final flats

tion parameters are presented in Table 3. In all cases the specimens failed in the base metal with properties similar to typical wrought Ti-6Al-4V weldments. Longitudinal bend tests (Table 4) showed that the fusion zone was the initiation site for fracture. As the bending strain was increased, the cracks grew outward through the HAZ and base metal—Fig. 6.

The slow bend precracked fracture toughness results are also presented in Table 3. It can be seen that both the fusion zone and HAZ exhibited superior toughness to the alpha-beta HIP base metal and inferior values to the beta HIP compacts. Although a direct quantitative comparison of these data cannot be made since the base metal specimens were of a different thickness (standard Charpy size of 0.394 in. as opposed to 0.125 in.), the trend that was exhibited has been previously reported (Ref. 6) for alpha-beta processed versus beta processed (heated above beta transus) material.

In most cases the welding of HIP specimens presented no problems when compared to Ti-6Al-4V wrought product. Figures 7 and 8 are montages of the microstructures of weldments of REP and H/DH compacted powders, respectively. As would be expected, the fusion and near heat-affected zones of each are similar. However, large differences did occur in the middle and far HAZ; these are discussed later.

Although there was no difference in the fusion zone microstructures of the two powder types, there was considerable difference in the tendency for void formation. Porosity was encoun-

Fig. 6—Crack initiation during longitudinal bend test. ×7 (reduced 46% during reproduction)

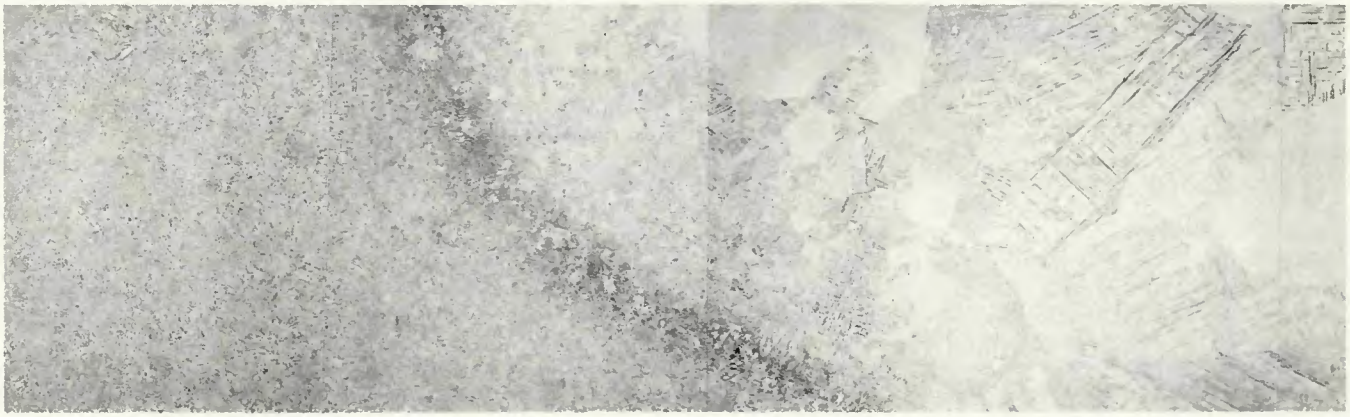

Fig. 7—Montage of weld in R3. ×35 (reduced 33% on reproduction)

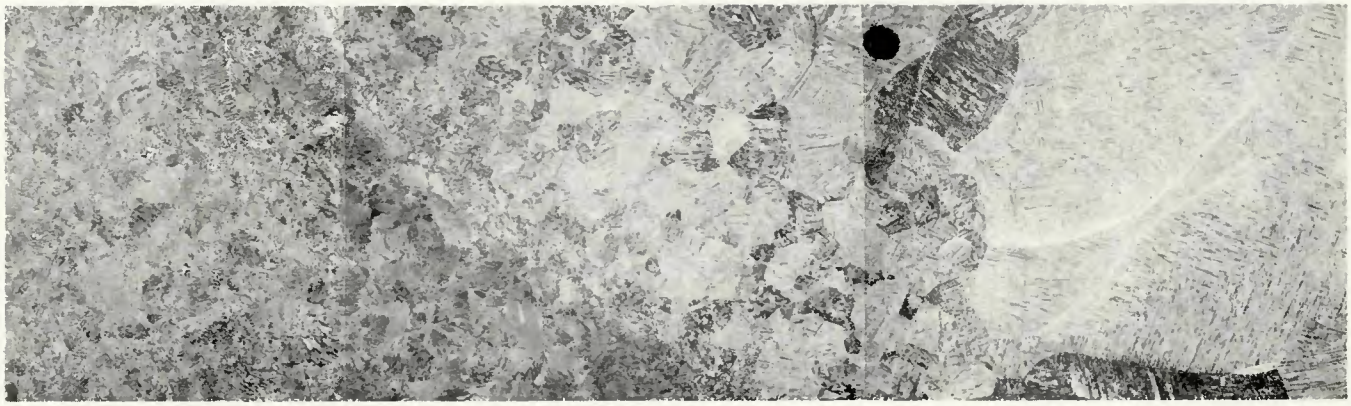

Fig. 8—Montage of weld in H/DH7. ×35 (reduced 33% on reproduction)

tered in all H/DH welds although compacts H/DH6 and H/DH7 were determined to be fully dense.

Figure 9 is a typical radiograph of a weld on a H/DH compact. It can be seen that the occurrence of this porosity was not the result of poor weld process control, since no voids are evident in the starting and stopping wrought Ti-6Al-4V tabs. Likewise, no porosity was encountered in fully dense REP compacts.

Discussion

It became apparent during this investigation that density determinations of compacted powders alone were insufficient to describe the material's weldability. Fully dense material, as determined volumetrically can still have porosity or lack of bonding at the individual particle interfaces in the base material.

Although this type of defect was very fine (and not observable optically), the stresses and heat supplied during welding were sufficient for voids of large diameter to form, presumably by coalescence, in the fusion zone. In the instances where porosity was more extensive, as in the case of material measured volumetrically as 99.9% dense, it made the material unweldable due to outgassing in the fusion zone with the resultant lack of penetration. This is clearly shown on the welds of compact H/DH5, a montage of which is shown in Fig. 10. A quantitative image analysis (using a Quantimet Model 720) of the base metal region of Fig. 10 showed 2.7 ± .5% porosity. During welding, the arc became unstable and, as shown in Fig. 12 erratic penetration resulted in a very poor underbead.

In order to rationalize these results, it is necessary to discuss the relative ease of compaction of these two different types of powders. Compacted under the same conditions, R1 and H/DH5 achieved different densities as previously noted. The fact that REP can achieve vibrated packing densities of greater than 65% of the theoretical density and that H/DH powder with 51% vibrated density, required cold isostatic compaction prior to HIP to achieve a comparable density is indicative of the effect of shape and, to a lesser extent, particle size distribution on achievable packing.

Fig. 9—Radiograph of weld in H/DH compact

The H/DH powder typically has a B.E.T. surface area of 0.060 m^2/g as opposed to a value of 0.009 m^2/g for the REP powder (Ref. 7). This six-fold difference in surface area is particularly significant in titanium alloys where the tendency for contamination by gas adsorption/absorption readily occurs. These differences in particle shape and specific surface area affect compaction and later the tendency for void formation during welding.

The base microstructures of both types of powder compacts from the 1700 F/8000 psi/3 h HIP cycle are shown in Fig. 12. The hydride-dehydride compact in Fig. 12a shows irregular boundaries at the particle interfaces with evidence of recrystallized equiaxed alpha. In addition, stored work is evident as seen by the bending of the acicular platelets showing that the powder has mechanically deformed as it joined together during cold compaction or early in the HIP cycle. This is less evident with the R3 compact (Fig. 12b) where an apparently strain free acicular structure with very few prior particle interfaces is seen.

Linear porosity in the fusion zone adjacent to the heat-affected zone was always observed in compacts of H/DH powder. In order to determine that this porosity was not a result of residual hydrogen, a special blank was welded and then dehydrided in a vacuum furnace at 1500 F (816 C) for 6 h. A second weld was made on the same plate, and it can be seen in the radiograph (Fig. 13) that the porosity was still evident. It is unlikely that hydrogen is the cause of this porosity. In fact, chemical analysis showed that the second pass was made when the total hydrogen content of the plate was only 27 parts per million.

The origin of the linear porosity in the weld zone is believed due to adsorbed gases, other than hydrogen, on these very high specific surfaces. The linear porosity encountered in H/DH compacts did not appreciably affect the properties measured in this investigation; however, it is anticipated that property degradation would have occurred if fatigue tests had been performed.

The fracture toughness in the heat-affected zone and fusion zones in all but the R4 beta processed compact showed higher values than the base material, as mentioned earlier. This was not an effect of the powder. It was instead a result of the change in microstructure from that of equiaxed alpha grains to a more acicular structure.

In the R4 compact, since the entire material was beta processed and exhibited an acicular structure (Fig. 14), the fracture toughness of the heat-affected and fusion zones was slightly lower because the rapid cooling rates in these zones did not allow the platelets to grow to sufficient thickness for optimum toughness (Ref. 8).

The effect of the microstructure produced during the welding operation and the subsequent rapid cooling can be further seen in Fig. 15. Microhardness traverses across welded powder and wrought material showed similar characteristics. In all cases the fusion and heat-affected zones possessed higher hardness than the base material. This is not due to oxygen absorption during welding since chemical analysis showed virtually no change in oxygen level across the

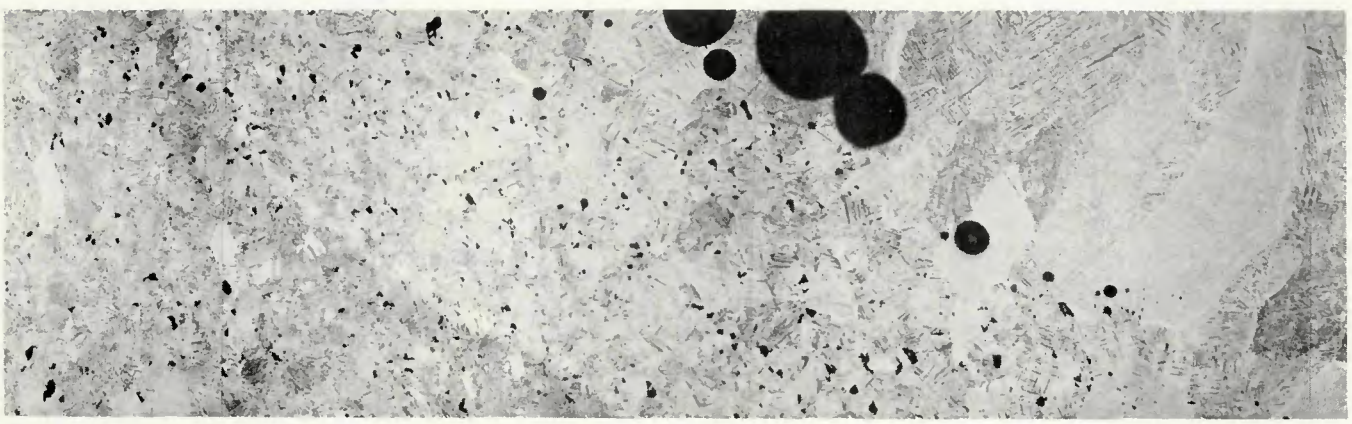

Fig. 10—Montage of weld in H/DH5. ×35 (reduced 33% on reproduction)

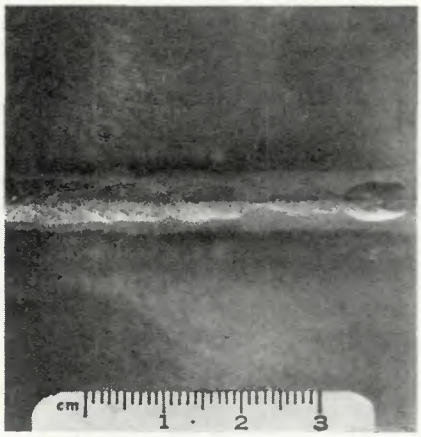

Fig. 11—Erratic penetration in H/DH5

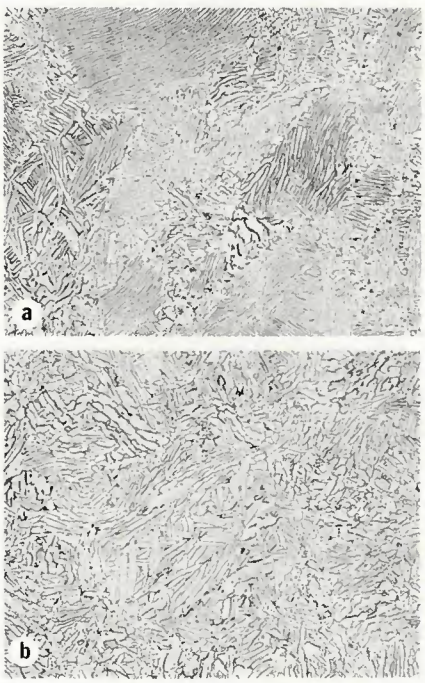

Fig. 12—Base microstructure of powder compacts: Top (a)—H/DH; bottom (b)—REP ×200 (reduced 50% on reproduction)

weldment. The higher hardness was a direct result of the finer transformation structure exhibited in these regions. The higher hardness and resultant lower toughness of these regions promoted crack formation in the fusion zone during the bend tests and the subsequent failures.

Conclusions

This study has shown that rotating electrode process (REP) powder consolidated by hot isostatic pressing (HIP) is weldable; whereas, hydride-dehydride (H/DH) process powder compacts consistently exhibited linear porosity in the fusion zone and hence may not be acceptable for some applications.

Of the two powder types evaluated, the REP powder appears less sensitive to the requirement for full density. The porosity encountered in the H/DH powder compacts, as exhibited before and after welding, is attributed to the high specific surface of the powder. However, porosity may also be attributed to the greater amount of adsorbed or absorbed gases and/or other contaminants which persist through the HIP cycle. Both powder types have acceptable as-welded tensile, bend, and toughness properties after HIP.

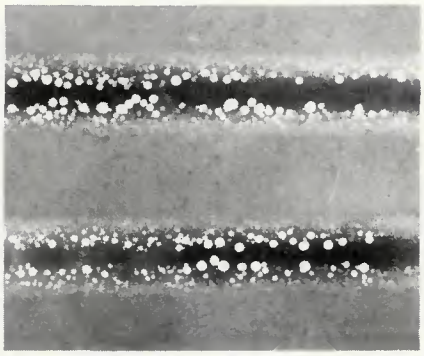

Fig. 13—Radiography of two-pass weld in H/DH compact (2nd pass lower)

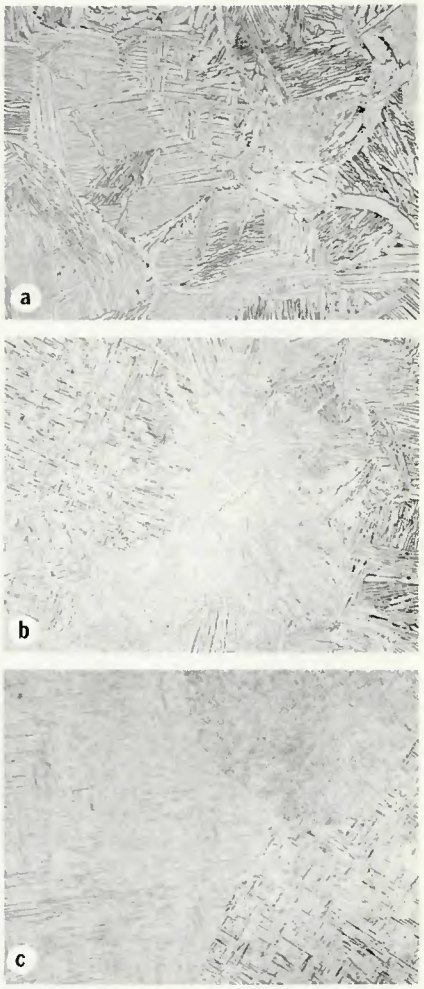

Fig. 14—Weld zones in beta processed compact R4. Left (a)—base material; middle (b)—HAZ; right (c)—fusion zone. ×200 (reduced 50% on reproduction)

References

1. Peebles, R. E., "Titanium Powder Metallurgy Forging," AFML-Technical Report TR-71-148, Wright Patterson AFB, Ohio 45433, September, 1971.

2. Witt, R. H. and Paul, O., "Potential Titanium Airframe Applications," *Powder Metallurgy for High Performance Applications*, Syracuse Press, 1972, p 333, presented at 18th Sagamore Army Materials Research Conference—Session on Powder Metallurgy for High Performance Applications, Raquette Lake, N.Y., September, 1971.

3. Geisendorfer, R. F., Sajdak, R. J. and Harth, G.H., "Hot Isostatic Pressing of Titanium 6Al-4V," *Titanium Science and Technology*, Vol. 1, New York, N.Y., 1973.

4. Peebles, R. E., "Hot Isostatic Pressing of Ti-6Al-4V Powder Forging Preforms," AFML Technical Report TR-75-5, Wright Patterson AFB, Ohio 45433, July, 1975.

5. Fleck, J. N., "Consolidation of Titanium Powder to Near-Net Shapes," Air Force Contract F33615-74-C-5114, AFML/LTM, Wright Patterson AFB, Ohio, 45433.

6. Coyne, J., *The Science Technology and Application of Titanium*, Pergamon Press, 1970, p. 97.

7. Friedman, G., "Development of Hot Isostatic Pressing Techniques for Producing High Quality Billet from Titanium Powder," AFML Technical Report TR-75-9, Wright-Patterson AFB, Ohio, July, 1975.

8. Greenfield, M. A., and Margolin, H., "The Interrelationship of Fracture Toughness and Microstructure in a Titanium Alloy," Met. Trans., Vol. 2, March, 1971, pp. 841-847.

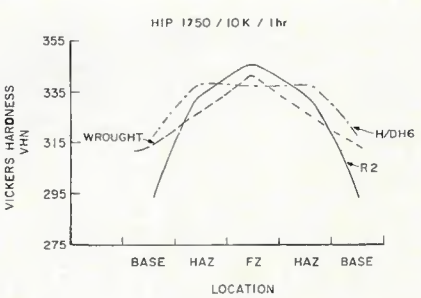

Fig. 15—Microhardness traverses across welded compacts